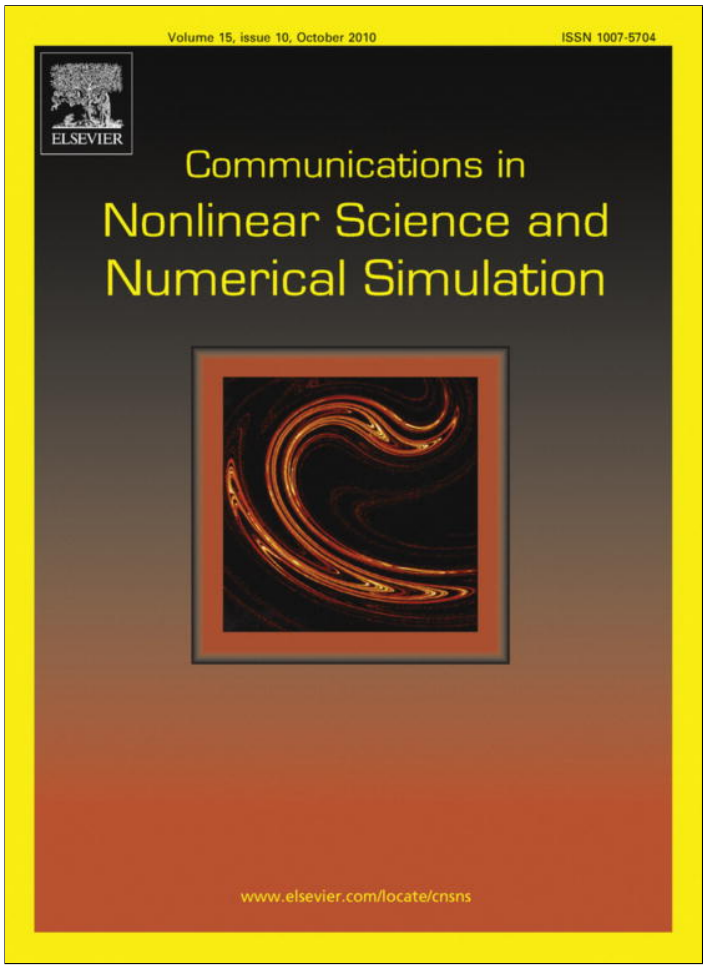

Commun Nonlinear Sci Numer Simulat 15 (2010) 3000–3014

Contents lists available at ScienceDirect

Commun Nonlinear Sci Numer Simulat

journal homepage: www.elsevier.com/locate/cnsns

Three-dimensional discrete-time Lotka–Volterra models with an application to industrial clusters

G.I. Bischi [a], F. Tramontana [b,*]

[a] Università degli Studi di Urbino, Dipartimento di Economia e Metodi Quantitativi, Via Saffi 42, 61029 Urbino, Italy
[b] Università Politecnica delle Marche, Dipartimento di Economia, Piazzale Martelli 8, 60121 Ancona, Italy

ARTICLE INFO

Article history:
Received 13 August 2009
Received in revised form 21 October 2009
Accepted 21 October 2009
Available online 27 October 2009

Keywords:
Discrete dynamical systems
Lotka–Volterra
Prey–predator
Bifurcations
Industrial economics

ABSTRACT

We consider a three-dimensional discrete dynamical system that describes an application to economics of a generalization of the Lotka–Volterra prey–predator model. The dynamic model proposed is used to describe the interactions among industrial clusters (or districts), following a suggestion given by [23]. After studying some local and global properties and bifurcations in bidimensional Lotka–Volterra maps, by numerical explorations we show how some of them can be extended to their three-dimensional counterparts, even if their analytic and geometric characterization becomes much more difficult and challenging. We also show a global bifurcation of the three-dimensional system that has no two-dimensional analogue. Besides the particular economic application considered, the study of the discrete version of Lotka–Volterra dynamical systems turns out to be a quite rich and interesting topic by itself, i.e. from a purely mathematical point of view.

1. Introduction

In the literature on applied mathematics there are many examples of dynamic models which have been developed for the description of physical or biological systems and then have been used, after suitable modifications, in order to describe the time evolution of economic, financial or social systems. For example, the Lotka–Volterra models, proposed by Lotka [1] for the description of chemical reactions and by Volterra [2] for the description of interacting populations, have also been used by Goodwin [3] as models of nonlinear endogenous oscillations in business cycle theory. Other examples can be found in evolutionary game theory, developed in biology and then usefully applied to describe economic and social interactions (see, among others, Hofbauer and Sigmund [4]). However, an important difference to be considered when dealing with dynamic modelling of economic systems is that economic time is often discontinuous (discrete) because decisions in economics cannot be continuously revised. In fact, discrete time is used because of the gap between decisions and realizations. Moreover, data are released, and consequently decisions are made, at discrete intervals (macroeconomic data like GDP, consumption or investments are annual, for example). For this reason discrete-time dynamical systems, represented by difference equations or, more properly, by the iterated application of maps, are often a more suitable tool for modelling dynamic economic processes. So, it is useful to study the peculiarities of discrete dynamical systems and their possible applications to economic dynamics.

* Corresponding author.
E-mail addresses: gian.bischi@uniurb.it (G.I. Bischi), f.tramontana@univpm.it (F. Tramontana).

1007-5704/$ - see front matter © 2009 Elsevier B.V. All rights reserved.
doi:10.1016/j.cnsns.2009.10.021

Even if in the Fifties and Sixties of the last century the methods for the study of iterated maps were less developed than those for ordinary differential equations, the situation is now rapidly changing. The dynamic properties and bifurcations of one-dimensional iterated maps are now quite well known, as well as their implications about periodic and chaotic behaviors of the trajectories (see e.g. [5–8]) and for two-dimensional maps more and more results can be found in the literature (see [9–12]).

The choice of discrete time dynamic models is also crucial because they may exhibit more complicated dynamic behaviors. Indeed, even in one-dimensional discrete dynamical systems represented by iterated quadratic maps, like the well known logistic map, periodic and chaotic trajectories can be easily observed. Analogously, two-dimensional discrete dynamical systems, in particular discrete time Lotka–Volterra equations, can exhibit a plethora of complicated asymptotic behaviors, from convergence to a fixed point or a periodic cycle until quasi-periodic motion along a closed invariant curve or even an erratic motion inside a bounded chaotic attractor (see e.g. [13,13–15]). Another problem which often arises in the study of nonlinear maps concerns the coexistence of several attracting sets, each with its own basin of attraction. In this case, a problem of equilibrium selection arises (see e.g. [16,17]) because the dynamic process becomes path-dependent, i.e. the kind of long run dynamics that is chosen depends on the initial condition. This opens the question of the delimitation of the basins of attraction and their changes as the parameters of the model vary. These two problems lead to two different routes to complexity, one related to the complexity of the attracting sets which characterize the long run time evolution of the dynamic process, the other one related to the complexity of the boundaries which separate the basins when several coexisting attractors are present. Both these questions require an analysis of the global dynamical properties, i.e. an analysis which is not based on the linear approximation of the map. When the map is noninvertible (i.e. "many-to-one") as it happens to be in the case of Lotka–Volterra quadratic maps, the global dynamical properties can be usefully characterized by the method of critical sets, a powerful tool introduced in the Seventies (see [10,18]) but only recently employed in the study of dynamic modelling of economic and financial systems (see e.g. [17,19,20]). The repeated application of a noninvertible map repeatedly folds the state space along the critical sets and their images, and often this allows one to define a bounded region where asymptotic dynamics are trapped. Conversely, the repeated application of the inverses "repeatedly unfolds" the state space, so that a neighborhood of an attractor may have preimages far from it. This may give rise to complicated topological structures of the basins, that can even be formed by the union of non-connected portions. The transition between two different topological structures of an invariant set (e.g. a chaotic attractor or a basin of attraction) are marked by global bifurcations due to contacts between different singular sets, such as contacts and crossings between stable sets and critical curves. The detection of these contact bifurcations are generally easily obtained in one-dimensional nonlinear maps, whereas in the study of two-dimensional maps an interplay between analytic, geometric and numerical methods is generally necessary, i.e. the occurrence of these contact bifurcations is shown by computer-assisted proofs (see e.g. [10] for many examples). An extension of such "modus operandi" to the study of higher dimensional noninvertible maps leads to nontrivial practical problems, related to the obvious reason that the computer screen is two-dimensional, so the visualization of objects in a phase spaces of dimension greater than two, and the detection of contacts among these objects as their shapes change, may become a very difficult task. In other words, the extension to higher-dimensional systems of the results on contact bifurcations, which gave so many interesting and promising results in the study of two-dimensional noninvertible maps, may become a very hard and challenging task, due to the difficulties met in the computer-assisted graphical visualization (see e.g. [21,22]).

In this paper we consider the following three-dimensional generalization of the discrete-time Lotka–Volterra dynamical system:

$$\begin{cases} x_1(t+1) = x_1(t)[e_1 + a_{11}x_1(t) + a_{12}x_2(t) + a_{13}x_3(t)] \\ x_2(t+1) = x_2(t)[e_2 + a_{21}x_1(t) + a_{22}x_2(t) + a_{23}x_3(t)] \\ x_3(t+1) = x_3(t)[e_3 + a_{31}x_1(t) + a_{32}x_2(t) + a_{33}x_3(t)] \end{cases}, \tag{1}$$

where the dynamic variables x_i represent the number of firms that produce homogeneous goods in an industrial cluster (or district) i, and the parameters e_i, a_{ij} are real variables, whose signs will be discussed in the following, that describe the interactions among the industrial clusters. We propose this model following a suggestion given by Fortis and Maggioni [23], who analyze different kinds of interactions between two clusters: the case of competition, mutualism (or symbiosis) and predation. The last case corresponds to a situation in which the growth of an industrial district is positively influenced by the presence of another one (producing complementary goods), whose growth is instead negatively influenced by the presence of a third cluster (producing substitutes). This may be the case of an industry located in a particular area which causes the birth of another correlated industry. However, if the younger industry is very productive, its growth could cause a crisis for the older one. Higher wages and new rates of interest, for example, may be not sustainable for the older industry. This is a typical prey–predator model in which the prey is the older industry. Fortis and Maggioni only analyze the case of two industrial districts, modelled by a two-dimensional Lotka–Volterra prey–predator model, and illustrate the occurrence of oscillatory dynamics. They also suggest that this situation could be extended to a model with more than two clusters, paying attention to the complexity that a higher dimensional model involves. We accept the challenge set by Fortis and Maggioni [23] by trying to move a first step towards the understanding of the dynamic behaviour of discrete Volterra models of dimension greater than two.

Three-dimensional discrete-time competitive Lotka–Volterra maps have been studied by Gardini et al. [24]. We try to extend their results to discrete-time prey predator models. We prove that these kinds of models give rise to global bifurcations that have no counterpart in the corresponding system of ordinary differential equations. For the three-dimensional discrete dynamical system analyzed in this paper we also show some numerical explorations which provide evidence for the existence of three-dimensional chaotic attractors, bounded by critical surfaces, as well as situations of coexisting attractors associated with non-connected basins. Even if the study of the contact bifurcations causing qualitative changes in the structures of three-dimensional attractors or basins are beyond the scope of the present paper, we want to stress how challenging is the extension of the graphical methods for the global dynamic analysis, currently used in two-dimensions, to the study of three-dimensional ones. It is plain that the dynamic situations analyzed in this paper constitute a first modest step towards the global analysis of three-dimensional discrete time Lotka–Volterra equations, and more generally it sheds some light on the properties of noninvertible three-dimensional maps.

It is hoped that this investigation will stimulate further studies on the dynamic properties of Lotka–Volterra maps in two and three dimensions and their numerous applications in the economic and social sciences.

The plan of the work is as follows. In Section 2 we recall some properties of two-dimensional Lotka–Volterra maps, in Section 3 we analyze the three-dimensional model and we show asymptotic behaviors and bifurcations which have a two-dimensional counterpart. In Section 4 we numerically show a bifurcation, which represents a particular kind of "route to chaos", with no two-dimensional counterpart. In Section 5 we describe some global properties and bifurcations related to noninvertibility of the iterated map, that can be studied by the method of critical curves in two dimensions, and we give some indications about their possible extensions to the three-dimensional model. Conclusions and suggestions for further research are given in Section 6.

2. The two-dimensional Lotka–Volterra map

In this section we recall some results about the two-dimensional Volterra map $T_2 : (x_1, x_2) \to (x_1', x_2')$ defined by

$$T_2 : \begin{cases} x_1' = x_1(e_1 + a_{11}x_1 + a_{12}x_2) \\ x_2' = x_2(e_2 + a_{21}x_1 + a_{22}x_2) \end{cases} \tag{2}$$

where the sign of the real parameters a_{ij} determine the kind of interaction (predation, competition or symbiosis). The discrete dynamical system (2) for competing species, i.e. with $a_{ij} \leqslant 0,\ i,j = 1,2$, has been considered by Blackmore et al. [13,13], where the coexistence of two locally stable equilibria is shown, as well as the presence of chaotic behaviors. Instead, we assume $a_{ii} \leqslant 0,\ i = 1,2$, (intra-specific competition) and $a_{ij}a_{ji} < 0,\ i,j = 1,2, i \neq j$ (prey–predator inter-specific relation). The dynamic properties of the trajectories generated by the iterated application of the map (2) have been recently studied by Liu and Xiao [14,15] in the particular case $e_1 = 1 + \delta r,\ e_2 = 1 - \delta d,\ a_{11} = -\delta r,\ a_{22} = 0,\ a_{21} = -a_{12} = \delta b$, where $\delta,\ r,\ d,\ b$ are positive parameters, and they show that the discrete dynamic model they consider can exhibit a plethora of complicated asymptotic behaviors, from convergence to a fixed point or a periodic cycle to quasi-periodic motion along a stable closed invariant curve or even an erratic motion inside a bounded chaotic attractor. In the rest of this section we recall some properties of the map (2) that may be useful to better appreciate the results about the three-dimensional model considered in the next section.

The map (2) admits four fixed points

$$\begin{aligned} &P_0 = (0,0); \quad P_1 = \left(\frac{1-e_1}{a_{11}}; 0\right); \quad P_2 = \left(0; \frac{1-e_2}{a_{22}}\right) \\ &Q = (x_1^*, x_2^*) = \left(\frac{a_{12}(e_2-1) + a_{22}(1-e_1)}{a_{11}a_{22} - a_{12}a_{21}}; \frac{a_{21}(e_1-1) + a_{11}(1-e_2)}{a_{11}a_{22} - a_{12}a_{21}}\right). \end{aligned} \tag{3}$$

Of course, both in ecological and economic applications only non-negative coordinates are meaningful. It is important to notice that the coordinate axes $x_i = 0,\ i = 1,2$, are trapping (invariant) sets, that is, any trajectory starting with initial condition $x_i(0) = 0$ remains trapped inside the same axis, i.e. $x_i(t) = 0$ for each $t \geqslant 0$, and is governed by the one-dimensional restriction of the map (2) to that axis, given by the quadratic one-dimensional map $x_j' = x_j(_j + a_{jj}x_j)$, topologically conjugate to the well-known logistic map $z' = \mu z(1-z)$ (see e.g. [5]) with parameter $\mu = e_j$ by the linear transformation $x_j = -\frac{e_j}{a_{jj}}z$. It is straightforward to realize that the fixed points of (2) located on the invariant coordinate axes are associated with the fixed points of the corresponding logistic restrictions.

The local stability of the fixed points of the map (2) is determined by the localization, in the complex plane, of the eigenvalues of the Jacobian matrix

$$J_2(x_1, x_2) = \begin{bmatrix} e_1 + 2a_{11}x_1 + a_{12}x_2 & a_{12}x_1 \\ a_{21}x_2 & e_2 + 2a_{22}x_2 + a_{21}x_1 \end{bmatrix} \tag{4}$$

i.e. the roots of the characteristic equation $F_2(\lambda) = \lambda^2 - Tr \cdot \lambda + Det = 0$, where Tr and Det represent, respectively, the trace and the determinant of the Jacobian matrix computed at the fixed points. The eigenvalues of the fixed points located along the invariant coordinate axes are always real. In fact, $J_2(P_0)$ is diagonal and the eigenvalues are the diagonal entries $\lambda_1 = e_1$

and $\lambda_2 = e_2$, with the corresponding eigendirections along the invariant axes, whereas $J_2(P_i),\ i = 1,2$, is a triangular matrix, so also in this case the eigenvalues are the diagonal entries $\lambda_1 = 2 - e_i,\ \lambda_2 = e_j + \frac{1-e_i}{a_{ii}} a_{ji},\ j \neq i$, with eigendirections along the invariant axis $x_j = 0$ and transverse to it respectively.

From these arguments the stability conditions for the three equilibria $P_i,\ i = 0,1,2$, are easily obtained:

P_0 is a stable node if $-1 < e_i < 1,\ i = 1,2$, a saddle point if $-1 < e_i < 1$ and $|e_j| > 1$ and an unstable node if $|e_i| > 1,\ i = 1,2;\ P_i,\ i = 1,2$, is stable along the corresponding invariant axis if $1 < e_i < 3$ (the well-known stability condition for the logistic restriction) and it is also transversely stable provided that

$$-1 < \frac{a_{ii}e_j + (1-e_i)a_{ji}}{a_{ii}} < 1$$

i.e.

$$a_{ii}(e_j - 1) + a_{ji}(1 - e_i) > 0$$
$$a_{ii}(e_j + 1) + a_{ji}(1 - e_i) < 0$$

where, since $a_{ii} < 0$, a change of sign of the left hand side of the first inequality represents a transcritical bifurcation (stability exchange at which $P_i \equiv Q$) and a change of sign of the left hand side of the second inequality represents a flip bifurcation transverse to the coordinate axis.

Finally, let us consider the stability conditions for the interior fixed point Q. The Jacobian matrix computed at Q is

$$J_2(Q) = \begin{bmatrix} 1 + a_{11}x_1^* & a_{12}x_1^* \\ a_{21}x_2^* & 1 + a_{22}x_2^* \end{bmatrix} \tag{5}$$

where the equilibrium conditions $e_1 + a_{11}x_1^* + a_{12}x_2^* = 1$ and $e_2 + a_{21}x_1^* + a_{22}x_2^* = 1$ have been used. In this case $Tr = 2 + a_{11}x_1^* + a_{22}x_2^*$ and $Det = (1 + a_{11}x_1^*)(1 + a_{22}x_2^*) - a_{12}a_{21}x_1^*x_2^*$. We first notice that the necessary stability condition

$$F_2(1) = 1 - Tr + Det = (a_{11}a_{22} - a_{12}a_{21})x_1^*x_2^* \geqslant 0$$

is satisfied, under our assumptions on the parameters, whenever the equilibrium Q is positive (i.e. where $x_1^*,\ x_2^* > 0$). Moreover, if $x_1^* = 0$, i.e. $a_{12}(e_2 - 1) + a_{22}(1 - e_1) = 0$, then $Q \equiv P_2$, corresponding to the transcritical bifurcation at which the transverse stability of P_2 is exchanged with that of Q, and $x_2^* = 0$ corresponds to the transverse transcritical bifurcation of P_1.

The other two stability conditions $F_2(-1) = 1 + Tr + Det > 0$ and $Det < 1$, such that a change of sign of a left hand side corresponds to a stability loss of Q via a flip and a Neimark–Sacker bifurcation[1] respectively, are more involved, a detailed analysis of them can be found in Liu and Xiao [14], even if they refer to a particular configuration of the parameters, as argued above. For the purposes of this paper, we just show some numerical explorations that show the occurrence of these two kinds of bifurcations. However, it is also worth noticing that the eigenvalues of the Jacobian matrix are complex provided that $Tr^2 - 4Det < 0$, and after some algebraic manipulation this condition becomes

$$(a_{11}x_1^* - a_{22}x_2^*)^2 + 4a_{12}a_{21}x_1^*x_2^* < 0 \tag{6}$$

from which it is evident that a necessary condition for (6) is:

$$4a_{12}a_{21}x_1^*x_2^* < 0$$

So, if the fixed point Q has positive coordinates, this condition is fulfilled only if $a_{12}a_{21} < 0$, i.e. under the assumption of a predator–prey relationship. In other words, a Neimark–Sacker bifurcation can only occur for a predator–prey model, and it is ruled out in the cases of competition or symbiosis.

A stable closed invariant curve, created after a *supercritical* Neimark–Sacker bifurcation of the map (2) is represented in Fig. 1(a). Another peculiarity of discrete time models is the existence of an infinite number of periodicity regions in the parameters plane (called *Arnold tongues*) near a Neimark–Sacker bifurcation (see e.g. [9,11]). This means that varying the values of one or more parameters may result in the sudden appearance of a periodic cycle whose periodic points are located along the closed invariant curve. This is the phenomenon of *phase locking* (see Kuznetsov [11, p. 272], for a detailed explanation). For instance, in Fig. 1(b) a situation is shown in which an attracting 6-cycle appears along the closed invariant curve as a consequence of a slight increase of the parameter a_{12}. By increasing further the parameter a_{12} we can see that the 6-cycle becomes a 12-cycle via flip bifurcation (Fig. 1(c)) and then a 24-cycle, etc.

Another interesting local bifurcation is observed if we consider the attracting 5-cycle of Fig. 1(d) and we decrease the value of a_{21}. In this case the points of the cycles undergo a supercritical Neimark–Sacker bifurcation giving rise to an attractor made up of five closed curves (Fig. 1(e)).

[1] The analogue, in discrete time, of the Hopf bifurcation in flows. In the supercritical case it gives rise to a closed and locally attractive invariant curve, on which periodic or quasi-periodic motion takes place.

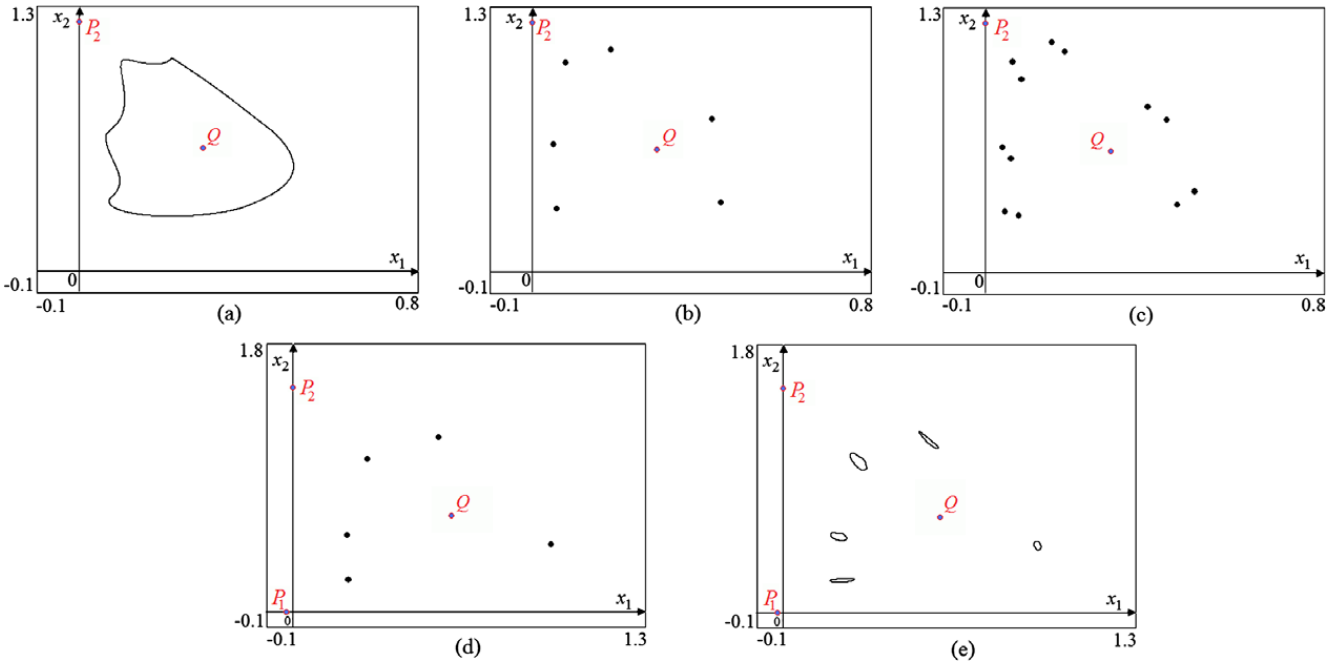

Fig. 1. (a) $e_1 = 0.321,\ e_2 = 2.56,\ a_{11} = -2.082,\ a_{12} = 2.12,\ a_{21} = -2.74,\ a_{22} = -1.24$, (b) $a_{12} = 2.14$, (c) $a_{12} = 2.16$, (d) $e_1 = 0.976,\ e_2 = 3.115,\ a_{11} = -1.44,\ a_{12} = 1.345,\ a_{21} = -2.13,\ a_{22} = -1.36$ and (e) $a_{21} = -2.16$.

3. The three-dimensional map

In this section we consider the three-dimensional model (1), generated by the repeated application of the map $T_3 : (x_1, x_2, x_3) \to (x_1', x_2', x_3')$ defined by

$$T_3 : \begin{cases} x_1' = x_1(e_1 + a_{11}x_1 + a_{12}x_2 + a_{13}x_3) \\ x_2' = x_2(e_2 + a_{21}x_1 + a_{22}x_2 + a_{23}x_3) \\ x_3' = x_3(e_3 + a_{31}x_1 + a_{32}x_2 + a_{33}x_3) \end{cases} \tag{7}$$

with the conditions on the parameters: $a_{ii} \leqslant 0,\ i = 1,2,3$, and $a_{i,j}a_{j,i} < 0,\ i,j = 1,2,3,\ i \neq j$, that can be seen as a generalization of the two-dimensional prey–predator Volterra map considered in the previous section.

Following Fortis and Maggioni [23] the map (7) is used to represents the time evolution of three industrial districts, such that the firms of each district produce homogeneous goods whereas the products of different districts may be linked by relations of substitutability or complementarity that can be described in terms of ecological interactions between animal populations, so that also the parameters can be interpreted as "intrinsic growth" or "intraspecific" or "interspecific" competition, as well as "hunting ability" or "nutritious capacity" of a cluster.

Analyzing the map (7) it is easy to realize that the coordinate axes are invariant sets. For example, if $x_1(0) = 0$ and $x_2(0) = 0$ then $x_1(t) = 0$ and $x_2(t) = 0$ for each $t \geqslant 0$, i.e. a trajectory starting on the x_3 axis remains trapped inside the same axis and is governed by the one-dimensional restriction of (7) to it, given by the quadratic map $x_3' = x_3(e_3 + a_{33}x_3)$. The same occurs for the other coordinate axes, as well as the coordinate planes. In fact, if $x_3(0) = 0$ then $x_3(t) = 0$ for each $t \geqslant 0$, i.e. a trajectory starting on the coordinate plane x_1x_2 remains there forever, and is governed by the two-dimensional map (2). Of course the same occurs for the other coordinate planes.

According to these invariance properties, it is easy to realize that the map (7) has eight equilibrium points, seven of which have at least one vanishing component: the origin $O = (0,0,0)$, three equilibria along the coordinate axes, given by $P_1 = (-e_1/a_{11}, 0, 0),\ P_2 = (0, -e_2/a_{22}, 0)$ etc., that can be denoted as one-clusters equilibria, three two-clusters equilibria Q_{ij} with one vanishing component, i.e. located on the coordinate planes, each corresponding to the Q of the map (2), and finally a unique equilibrium R (coexistence-equilibrium) whose coordinates are given by the solution of an algebraic system of three linear equations. Of course, these equilibria are meaningful (and really represent coexistence of clusters) only when their nonvanishing components are positive.

The conditions for the local stability of the equilibria are obtained through the localization, in the complex plane, of the eigenvalues of the Jacobian matrix

$$J_3 : \begin{bmatrix} e_1 + 2a_{11}x_1 + a_{12}x_2 + a_{13}x_3 & a_{12}x_1 & a_{13}x_1 \\ a_{21}x_2 & e_2 + 2a_{22}x_2 + a_{21}x_1 + a_{23}x_3 & a_{23}x_2 \\ a_{31}x_3 & a_{32}x_3 & e_3 + 2a_{33}x_3 + a_{31}x_1 + a_{32}x_2 \end{bmatrix} \tag{8}$$

computed at the fixed points.

Also in this case the equilibrium with all positive coordinates is the most interesting one, because its stability ensures long-run coexistence of all the industrial districts.

In order to check the local stability of the coexistence-equilibrium R we have to look at the characteristic polynomial of the Jacobian matrix calculated at R, which takes the form:

$$F_3(\lambda) = \lambda^3 + A_1\lambda^2 + A_2\lambda + A_3 = 0 \tag{9}$$

Following Farebrother [25] necessary and sufficient conditions for R to have all the eigenvalues less than one in modulus are the following (equivalent conditions can be found in Gandolfo [26]. Yury's conditions in Elaydi [27] and in Okuguchi and Irie [28]):

$$\begin{aligned} &\text{(i)} \quad 1 + A_1 + A_2 + A_3 > 0,\\ &\text{(ii)} \quad 1 - A_1 + A_2 - A_3 > 0,\\ &\text{(iii)} \quad 1 - A_2 + A_1A_3 - (A_3)^2 > 0,\\ &\text{(iv)} \quad A_2 < 3. \end{aligned} \tag{10}$$

In our case the coefficients of the characteristic polynomial (9) are not suitable to easy algebraic manipulation, so it is an hard task to obtain analytic conditions on the parameters for the local stability of R and related local bifurcations. In what follows we numerically explore the main local bifurcations of the fixed points and other invariant sets. As we shall see, even in the case of instability of the positive equilibrium R coexistence of clusters can be obtained as well, provided that other kinds of attracting sets exist in the positive orthant, such as stable periodic cycles or stable closed invariant curves or chaotic attractors. These different kinds of positive attractors give rise to interesting time evolutions of the clusters, characterized by oscillatory dynamics. This means that it is possible to obtain an alternation of periods in which one (or more) cluster(s) are more numerous than the other(s) as well as periods in which all clusters are formed by a high number of firms or by only a few firms, and all these situations are generated endogenously.

Conditions for the disappearance (or "extinction") of one industrial cluster are obtained through the study of the transverse stability of the *boundary equilibria*, that is equilibrium points (or more complex attractors) located in the invariant coordinate planes in which only two clusters are present, as shown in Appendix A.

In the reminder of this section we show some examples where the dynamic situations, in particular the attracting sets observed, are very similar to the ones already seen for the two-dimensional model.

3.1. Flip and Neimark–Sacker bifurcations

The presence of a closed locally attractive invariant curve located in the positive orthant means that we can have coexistence of clusters, but the number of firms belonging to each cluster oscillates from one period to another. Situations like those shown in Fig. 1 are interesting because they represent conditions of coexistence of different clusters, even if the equilibrium R is unstable: each cluster will survive under these conditions. The same kind of bifurcations can occur with three clusters, as we now show by some numerical explorations of a simplified version of the three-dimensional map (7) in which the parameters can be subdivided in groups with the same value, emphasizing similarity among clusters: they grow at the same speed because $e_1 = e_2 = e_3$ and $a_{11} = a_{22} = a_{33}$; they also have the same *nutritious capacity* and the same *hunting ability*, because $a_{12} = a_{31} = a_{23}$ and $a_{13} = a_{21} = a_{32}$. In Fig. 2 (a) we can see a stable closed invariant curve appeared after a supercritical Neimark–Sacker bifurcation at which the positive equilibrium R becomes unstable. In Fig. 2(b) we can notice the appearance of a stable 12-cycle with periodic points located along the closed invariant curve, a typical phase-locking phenomenon when the parameters enter an Arnold tongue. Changing the common value of the parameters a_{13}, a_{21} and a_{32} a first flip bifurcation occurs and the 12-cycle becomes unstable generating, at the bifurcation, a stable 24-cycle (Fig. 2(c)), then a sec-

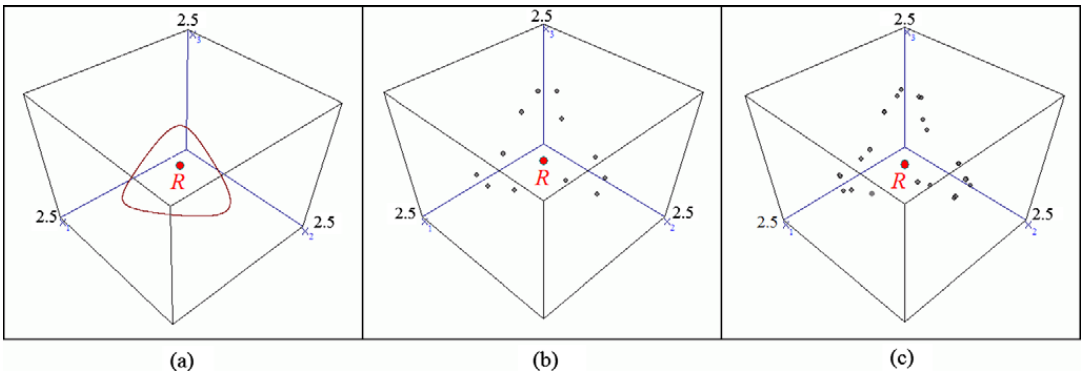

Fig. 2. (a) $e_1 = e_2 = e_3 = 2$, $a_{11} = a_{22} = a_{33} = -1$, $a_{12} = a_{31} = a_{23} = 0.61$, $a_{13} = a_{32} = a_{21} = -0.5$, (b) $e_1 = e_2 = e_3 = 2$, $a_{11} = a_{22} = a_{33} = -1$, $a_{12} = a_{31} = a_{23} = 1.1$, $a_{13} = a_{32} = a_{21} = -0.98$ and (c): $a_{13} = a_{32} = a_{21} = -0.9713$.

ond flip bifurcation we have a 48-cycle and so on. In Fig. 2(c) it is quite evident that Fig. 2 shows a three-dimensional extension of the same phenomenon already present in the two-dimensional case Fig. 1. So increasing the number of clusters we do not exclude the possibility of coexistence even when the positive equilibrium is unstable.

4. A specific three-dimensional bifurcation: period doubling of closed invariant curves

In section 3 we have numerically shown some local bifurcations of the three-dimensional map (7), which can be considered similar to the bifurcations shown in Section 2 for the two-dimensional maps. In contrast, in this section we introduce a particular bifurcation of the three-dimensional model which cannot be observed in the two-dimensional case.

Fig. 3 is obtained by using the set of parameters used in Fig. 2(a) , except for the common value of $a_{12} = a_{31} = a_{23}$ which is used as a bifurcation parameter. Fig. 3(a) (where the value of the modified parameter is 0.65) shows a stable closed invariant curve created via a Neimark–Sacker bifurcation. By increasing the common value of the parameters to 0.6575 , we obtain the invariant closed curve shown in Fig. 3(b), so we can say that the curve undergoes a kind of "period doubling". In fact in Fig. 3(b) a unique invariant curve still exists but with a quasi-doubled period with respect to the curve represented in Fig. 3(a). If we further increase the value of the parameters we can see better that we continue to have only one curve (Fig. 3(c), obtained by using the value 0.665). When the value is 0.66824 we have a second period doubling of the closed invariant curve and we can see it in Fig. 3(d), as well as in the enlargements and rotations of the same attractor shown in Fig. 3(e)–(g).

It is worth noting that this bifurcation is not related to the period-doubling of periodic orbits in flows, but rather with the flip bifurcation in maps.

It is also interesting to stress that this sequence of bifurcations may lead to the creation of a chaotic attractor, like the one shown in Fig. 3(h) obtained with the value 0.675.

5. Towards other extensions of two-dimensional global properties to three dimensions

In this section we describe some global geometric properties and bifurcations of the two-dimensional Lotka–Volterra map (2) related to the fact that it is a noninvertible map (see Appendix B). An important problem in the study of applied dynamical systems is the delimitation of a bounded region of the state space where the system dynamics are ultimately trapped, despite the complexity of the long-run time patterns. This is useful information, often more useful than a detailed description of step by step time evolution. Another important question concerns the delimitation of the basins of attraction, and their qualitative changes, when several attractors coexist. Both these questions require an analysis of the global dynamical properties of the dynamical system, that is, an analysis which is not based on the linear approximation of the map. When the map is noninvertible, its global dynamical properties can be usefully characterized by using the formalism of critical sets, by which the folding action associated with the application of the map, as well as the "unfolding" associated with the action of the inverses, can be described. Loosely speaking, the repeated application of a noninvertible map repeatedly folds the state space along the critical sets and their images, and often this allows one to define a bounded region where asymptotic dynamics are trapped. As some parameter is varied, global bifurcations that cause sudden qualitative changes in the properties of the attracting sets can be detected by observing contacts of critical curves with invariant sets. In contrast, the repeated application of the inverses "repeatedly unfold" the state space, so that a neighborhood of an attractor may have preimages far from it, thus giving rise to complicated topological structures of the basins, that may be formed by the union of several (even infinitely many) non-connected portions. In fact, as explained in Appendix B, in order to study the extension of a basin and the structure of its boundaries one has to consider the properties of the inverse relation. The route to more and more complex basin boundaries, as some parameter is varied, is characterized by global bifurcations, also called contact bifurcations, due to contacts between the critical set and the invariant sets that form the basin boundaries.

For two-dimensional noninvertible maps, the determination of these *contact bifurcations* is often based on computer-assisted studies, carried out through a continuous dialog between analytic, geometric, and numerical methods, which often requires careful use of computer graphics. This creates some practical problems when one tries to generalize such methods to three dimensions, due to the difficulties in visualizing three-dimensional objects on the bidimensional computer screen. As a consequence, the detection of contacts among these objects, as their shapes change, may prove to be a very difficult and challenging task.

5.0.1. Non-connected basins of attraction

A problem that often arises in the study of nonlinear dynamical systems concerns the existence of several attracting sets, each with its own basin of attraction. In this case the dynamic process becomes path-dependent, i.e. the long run dynamics characterizing the system depends on the starting condition. In this section we show that this occurrence can be easily met in the study of Lotka–Volterra maps like (2) and (7). For example a stable fixed point can coexist with an attractive periodic cycle or with an attractive close invariant curve. In such situations of *multistability* it is important to understand the extension and the structure of the basins of attraction.

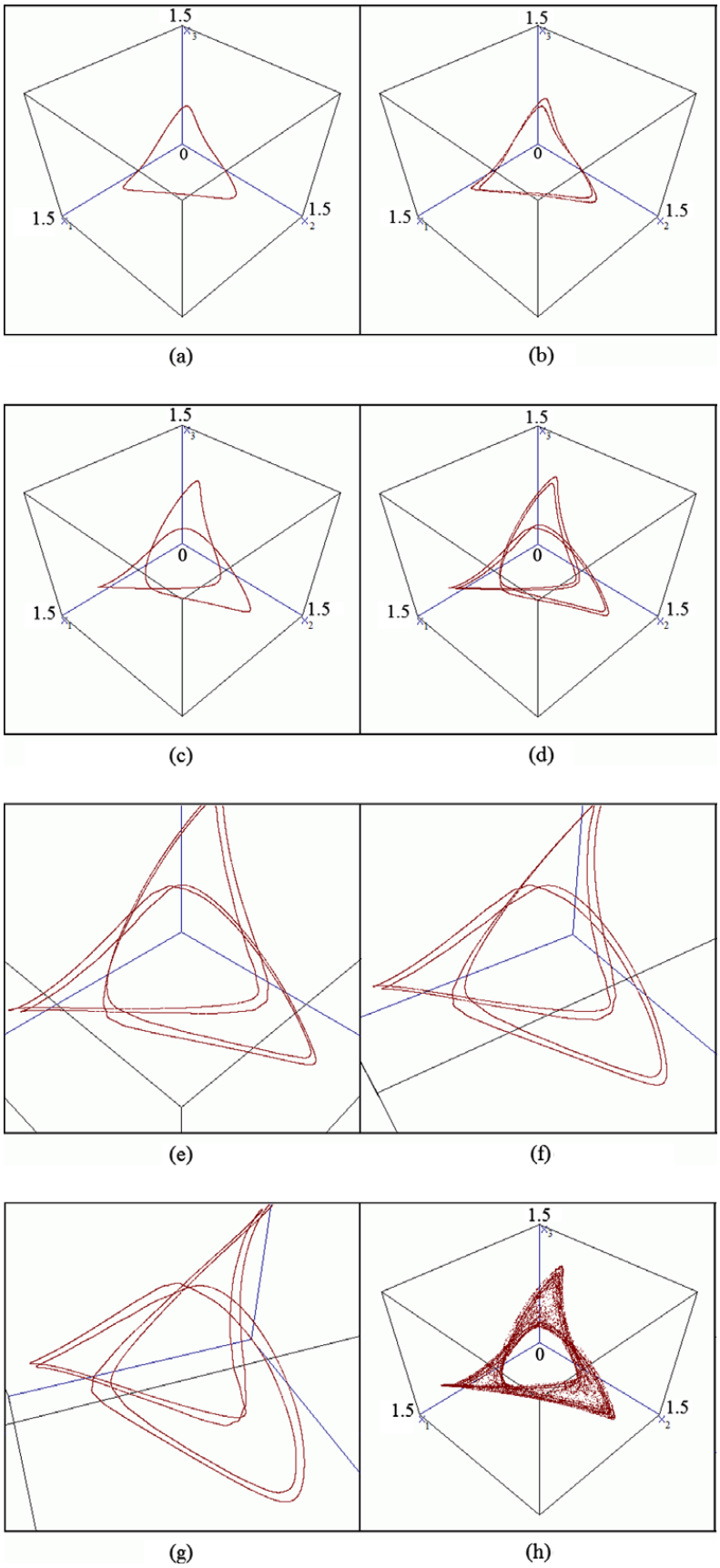

Fig. 3. Numerically computed trajectories of the three-dimensional map with the set of parameters used in Fig. 2 (a), except for the common value $a = a_{12} = a_{31} = a_{23}$ which is used as a bifurcation parameter. (a) $a = 0.65$; (b) $a = 0.6575$; (c) $a = 0.665$; (d) $a = 0.66824$; (e)–(g) show enlargements or rotations of picture (d) and (h) $a = 0.675$.

An example of multistability for the map (2) is given in Fig. 4, where we see coexistence between the locally attractive equilibrium Q and an attractive 2-cycle formed by the points C_1 and C_2 located on the horizontal axis. The yellow basin of attraction represents all the initial conditions leading to the coexistence equilibrium whereas the blue one represents the initial condition leading to the 2-cycle. The grey region is formed by initial conditions leading to infeasible trajectories that involve negative values of the state variable, hence without any economic meaning.

We can see that initial conditions which are very close to each other, and close to the boundary between the two basins, can lead to different attractors, which in this case means coexistence or not between clusters.

The three-dimensional case can exhibit multistability too. Fig. 5(a) shows a case of coexistence between a stable closed invariant curve and an attractive 6-cycle. In this case both the attractors represent a kind of coexistence among clusters. Fig. 5(b) shows a section of the two basins of attraction, red for the 6-cycle and yellow for the closed curve. Also in this situation, for trajectories starting very close to each other, the system may converge to different attractors.

This situation is more evident when we have non-connected basins of attraction, i.e. characterized by isolated portions nested inside another basin. These basins, besides the portion containing the attractor (called *immediate basin*) also include separated portions (that we can call *islands*). In 6(a) and (b) we have examples of this basins' configuration, for the map (2) and the map (7) respectively.

In order to explain the transition from connected to non-connected basins, we need to study the global properties of the dynamical systems by using the method of critical sets (see Appendix B).

In 7 we show the critical curves of our two-dimensional case. We can see that LC_{-1}, locus of points with vanishing Jacobian, is a parabola (the equation is given in Appendix B) whereas LC is formed by two branches that join in a cusp point. LC separates regions formed by points that have one or three distinct preimages.

Comparing Fig. 6(a) and Fig. 7 we can see that when the parameter a_{11} is decreased, the grey region near the lower branch of LC crosses the critical curve. Points that in Fig. 6(a) have crossed the curve now have three preimages instead of one, and in this way we can explain the non-connected grey "islands" nested inside the white basin. This can be stated by saying that by decreasing the value of the parameter a_{11} , a *global bifurcation* occurs that gives rise to more complex topological structures of the basins.

When we work with a three-dimensional map like (7), we have to extend the concept of *critical curves* to *critical surfaces*. It is quite complicated to obtain analytically and even to draw the *critical surfaces* but we can easily imagine that the disconnected portions of the grey basin represented in Fig. 6(b) are caused by a contact between the basin of infinity and a *critical surface*. The main practical problem is that the visualization of two-dimensional sections of the basins is not useful to detect

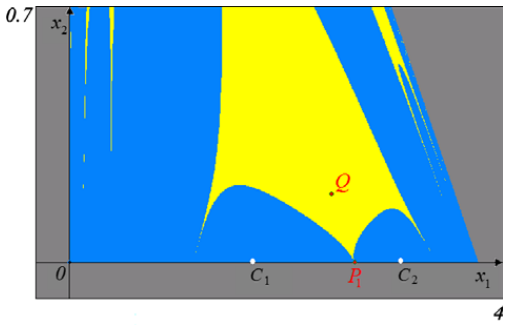

Fig. 4. Obtained by using the following set of parameters: $e_1 = 3.3,\ e_2 = -0.8,\ a_{11} = -0.88,\ a_{12} = -0.7,\ a_{21} = 0.75,\ a_{22} = 0$.

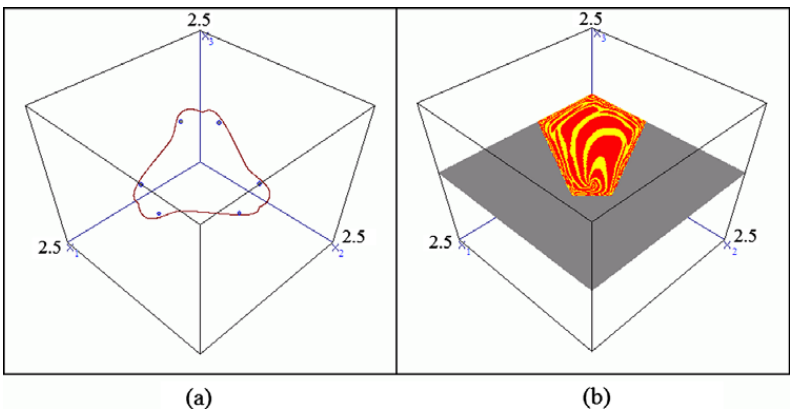

Fig. 5. Obtained by using the following set of parameters: $e_1 = e_2 = e_3 = 2.4,\ a_{11} = a_{22} = a_{33} = -1.4,\ a_{12} = a_{31} = a_{23} = 0.714,\ a_{13} = a_{32} = a_{21} = -0.5$.

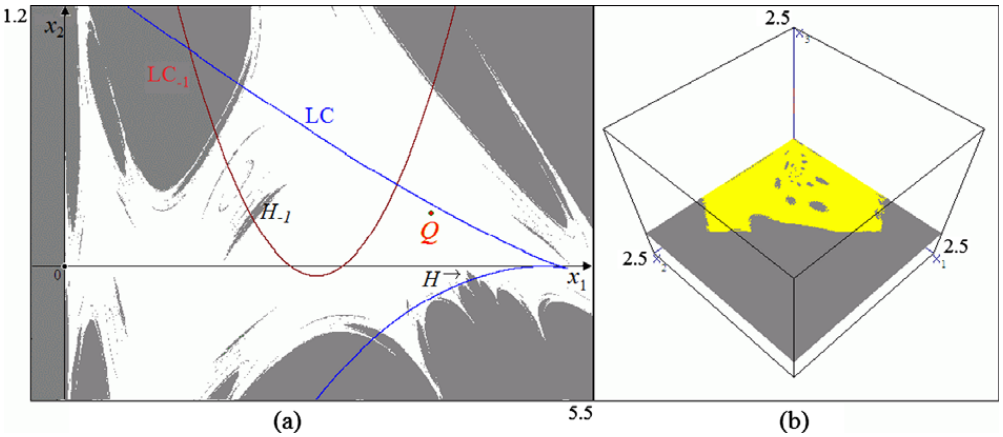

Fig. 6. (a) The white area is the basin of attraction of a chaotic attractor on the horizontal axis , whereas the grey region is the basin of the infinity where trajectories diverge: $e_1 = 3.57, e_2 = -1.6,\ a_{11} = -0.68,\ a_{12} = -0.7,\ a_{21} = 0.75,\ a_{22} = 0$ and (b) the yellow region is the basin of attraction of a chaotic attractor whereas the grey one has the same meaning seen in the two-dimensional case: $e_1 = e_2 = e_3 = 2.4,\ a_{11} = a_{22} = a_{33} = -1.4,\ a_{12} = a_{31} = a_{23} = 0.93,\ a_{13} = a_{32} = a_{21} = -0.5$. (For interpretation of references in color in this figure legend, the reader is referred to the web version of this article.)

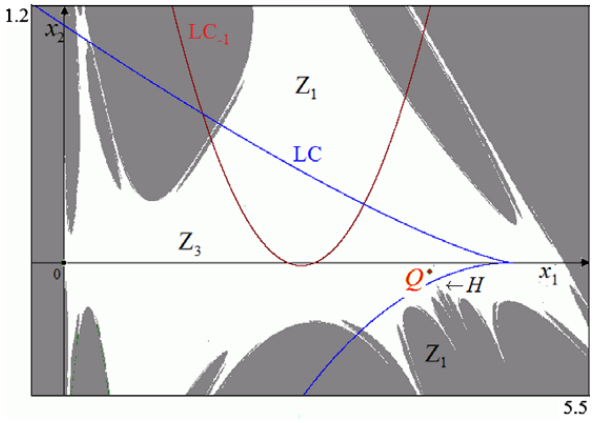

Fig. 7. Obtained by using the following set of parameters: $e_1 = 3.57,\ e_2 = -1.6,\ a_{11} = -0.75,\ a_{12} = -0.7,\ a_{21} = 0.75,\ a_{22} = 0$.

contacts. However, even using three-dimensional graphical representations, other difficulties arise related to the fact that it is necessary to visualize objects which are nested inside other objects. Some attempts to tackle this problem can be found in [21,22] where the problem of visualizing three-dimensional non-connected basins is approached by using sophisticated graphical programs in order to modulate the opacity of the outer objects in order "to see through" them. Moreover, the critical sets are now two-dimensional surfaces embedded in a three-dimensional phase space, and their contacts with portions of basin boundaries, also given by two-dimensional surfaces, may be very difficult to detect, unless the critical surfaces are represented like semi-transparent veils.

5.1. Chaotic attractors and their delimitation

As explained in Appendix B, the concept of critical curves has been often applied in two-dimensional discrete dynamical systems, represented by the iteration of noninvertible maps, in order to bound trapping regions inside which the asymptotic dynamics are included. In particular, portions of critical curves and their images can be used to obtain the boundaries of the chaotic attractors. This is important because it allows one to deduce the maximum (minimum) values that the endogenous variables may assume during the chaotic dynamics, that is in our case the maximum (minimum) number of firms observable for each cluster. In Fig. 8 we show examples of two-dimensional and three-dimensional chaotic attractors, obtained by the iteration of maps (2) and (7) respectively. If we want to obtain the boundaries of the two-dimensional *chaotic attractor* shown in Fig. 8(a), following the procedure given in Mira et al. [10] (see also Bischi and Gardini [29]) we need to consider the portion of LC_{-1} which is inside the attractor and the images of increasing order (denoted by $LC,\ LC_1,\ LC_2, \ldots$) until they form a closed boundary of a chaotic attractor, as shown in Fig. 9.

Even if we cannot draw portions of *critical surfaces* and their images, we know that the three-dimensional boundary of the *chaotic attractor* shown in Fig. 8(b and c) is formed by them, and can be obtained by using an iterative method like the one described above.

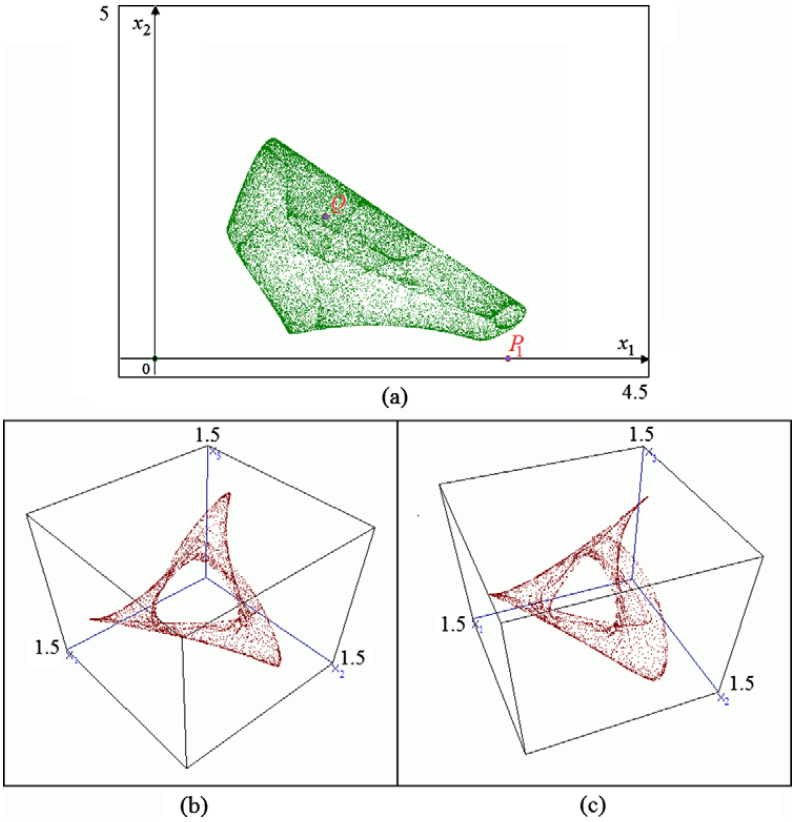

Fig. 8. (a) $e_1 = 3.7,\ e_2 = -0.4,\ a_{11} = -0.88,\ a_{12} = -0.7,\ a_{21} = 0.95,\ a_{22} = 0$. (b) and (c) represents the same chaotic attractor seen from two different points of view: $e_1 = e_2 = e_3 = 2,\ a_{11} = a_{22} = a_{33} = -1,\ a_{12} = a_{31} = a_{23} = 0.675,\ a_{13} = a_{32} = a_{21} = -0.5$.

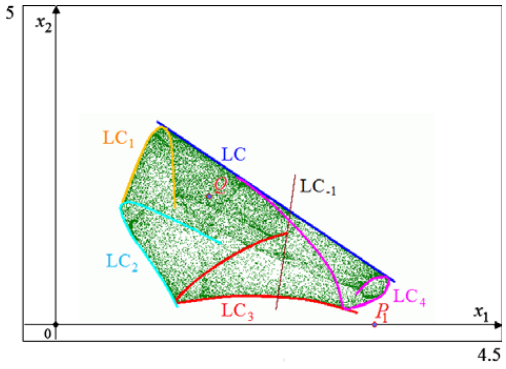

Fig. 9. This picture shows how the borders of the chaotic attractor of Fig. 8(a) can be obtained by *mapping* the portion of LC curve located inside the attractor itself.

6. Conclusions and further research

We have analyzed a three-dimensional version of the discrete-time prey–predator Lotka–Volterra model, motivated by an economic model suggested by Fortis and Maggioni [23] concerned with the interactions among industrial clusters. Predatory relations among industrial districts are also described in Dendrinos and Mullally [30], Nijkamp and Reggiani [31,32]: new industrial clusters are created as the result of spin-off and then the newborn clusters cause a decline of older ones.

The aim of this paper is twofold. First, it tries to model an important economic issue concerning the interaction of different industrial districts, producing goods that can be complements or substitutes, by using models and terminology typical of interacting populations in the ecologic literature. Results on coexistence of different species in ecologic environments can be usefully translated to the case of industrial clusters, in particular the case of oscillatory coexistence represented by periodic and chaotic attractors. Our results show that by increasing the number of districts producing homogeneous goods, and such that the development of one district causes the decline of another through a typical prey–predator relation, may increase the possibility of endogenous oscillations. The intrinsic difficulty in getting stationary coexistence of several industrial districts

does not necessarily imply the occurrence of competitive exclusion of some of them, because coexistence may persist even if it is characterized by oscillations. This situation can be managed by encouraging the transfer of workers and know-how from one district to another according to the observed ups and down. Similar conclusions are not new in ecologic modelling, see e.g. May [33]. In general, it would be useful to consider other possible kinds of interactions among industrial clusters, from mutualism to competition, in order to see what policies are more effective to enhance the possibility of coexistence, both stationary or oscillatory. Of course, the dynamic models for the description of more and more industrial clusters become more and more complicated. This paper takes a first modest step by stressing the effects of moving from two to three industrial clusters. Indeed, we have shown that the bifurcations observed in the two-dimensional version have a three-dimensional counterpart. However, one more dimension involves the possibility that new bifurcations occur, and an example is given in section 4.

Multistability is also shown, together with *non-connected basins*, to be peculiar to noninvertible maps. Complex structures of the attractors, as well as in the boundaries of the basins of attraction, are expected also in the study of other versions of the Lotka–Volterra three-dimensional model (2 preys–1 predator or 2 predators–1 prey), so a more complete analysis of the global dynamic properties of discrete-time Volterra models may give rise to further interesting results. What we propose in this note is just an exercise to show how complex dynamic behaviors and bifurcations can be observed in discrete-time three-dimensional models.

This leads to the second stream to which the present paper contributes, which is related to the study of the global properties of noninvertible maps by the method of critical sets (see e.g. [10,18,34] and references therein). Indeed, it is now sufficiently well-known that the creation of non-connected basins in one-dimensional noninvertible maps can be explained in terms of contacts between *critical points* and basin boundaries (also called *contact bifurcations*, see [6]). In recent years, in the study of two-dimensional noninvertible maps, analogous results have been obtained by the method of *critical curves*, a two-dimensional generalization of the notion of local maxima and minima in the one-dimensional case (see e.g. [10,34,35]). The extension of these methods to the study of models involving three-dimensional noninvertible maps, like the one considered in the present paper, is an almost unexplored field. For maps of dimension greater than one, explicit analytical expressions, in terms of elementary functions, of the critical sets, and of the basin boundaries involved in the contact bifurcations are generally not known. So, even for two-dimensional noninvertible maps, the methods followed in the determination of the *contact bifurcations* are based on a systematic computer-assisted study, carried out through a continuous dialog between analytic, geometric, and numerical methods, which often require a careful usage of computer graphics. This creates some nontrivial practical problems when one tries to generalize such methods to more than two dimensions. In fact, since the computer screen is two-dimensional, the visualization of objects in a phase space of dimension greater than two, and the detection of contacts among these objects as their shapes change, may prove a very difficult task. In other words, the extension to higher-dimensional systems of the results on contact bifurcations, which gave so many interesting and promising results in the study of two-dimensional noninvertible maps, may become a very hard and challenging task, due to the difficulties met in the computer-assisted graphical visualization. In Agiza et al. [36], two-dimensional sections are employed in order to visualize the basins of coexisting attractors, but this method is not useful to detect the occurrence of qualitative changes in the structure of the basins and the contact bifurcations which cause such changes. Indeed, in our case the problem of 3D visualization also involves other difficulties, related to the fact that it is necessary to visualize objects which are nested inside other objects. This means that sophisticated graphical programs are necessary in order to completely analyze such global bifurcations, see e.g. [21,22].

Appendix A. Coexistence of only two clusters in the three-dimensional model

In order to study the transverse stability of an invariant set embedded into a two-dimensional invariant coordinate plane, we have to analyze the Jacobian matrix of the map (7) in such a plane. Let us consider the case $x_3 = 0$ (mutatis mutandis the reasoning would be the same taking $x_1 = 0$ or $x_2 = 0$). The Jacobian matrix becomes:

$$\widetilde{J}_3 : \begin{bmatrix} e_1 + 2a_{11}x_1 + a_{12}x_2 & a_{12}x_1 & a_{13}x_1 \\ a_{21}x_2 & e_2 + 2a_{22}x_2 + a_{21}x_1 & a_{23}x_2 \\ 0 & 0 & e_3 + a_{31}x_1 + a_{32}x_2 \end{bmatrix}$$

where the eigenvalue regulating the transverse attractivity of the plane is explicitly given by the third element of the third line, that is:

$$\lambda_3(x_1, x_2) = e_3 + a_{31}x_1 + a_{32}x_2 \tag{11}$$

This means that if the fixed point $Q_{12} := (x_1^*, x_2^*)$ of the restriction of (7) to the invariant plane $x_3 = 0$ is locally stable according to the conditions given in Section 2, i.e. there exist a neighborhood of the point in the plane $x_3 = 0$ whose points converge asymptotically to Q_{12}, then if the transverse eigenvalue is such that $|\lambda_3(x_1^*, x_2^*)| < 1$ there also exists a neighborhood of Q_{12} outside the plane $x_3 = 0$, belonging to the basin of attraction of Q_{12}.

An example is given in Fig. 10 obtained by using the following set of parameters: $e_1 = 1.4,\ e_2 = 2.12,\ e_3 = 0.04,\ a_{11} = -2,\ a_{12} = 0.9,\ a_{13} = -0.43,\ a_{21} = -0.9,\ a_{22} = -0.88,\ a_{23} = 0.8,\ a_{31} = 1.8,\ a_{32} = -1.1$ and $a_{33} = -1.1$.

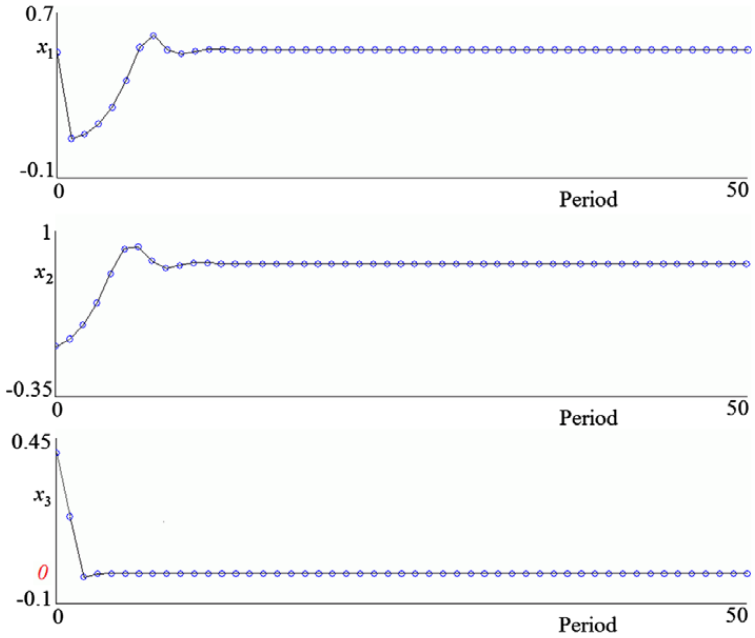

Fig. 10. The values of the three variables are plotted versus time. The asymptotic values of x_1 and x_2 are strictly positive, while the value of x_3 converges to 0.

In this case, in the two-dimensional subspace $x_3 = 0$, there exists a fixed point $Q_{12} = (0.529; 0.7915)$ locally stable starting from the trapping subspace. Moreover, the transverse eigenvalue is such that $\lambda_3(0.529; 0.7915) = 0.1233$.

Even other kinds of attractors (periodic, quasi-periodic or chaotic) for the trapping plane $x_3 = 0$ could be transversely attractive, but in these cases it could be more difficult to demonstrate it analytically.

Appendix B. Definition and computation of critical sets

A map $T : S \to S,\ S \subseteq \mathbb{R}^n$, defined by $\mathbf{x}' = T(\mathbf{x})$, transforms a point $\mathbf{x} \in S$ into a unique point $\mathbf{x}' \in S$. The point $\mathbf{x}'$ is called the *rank-1 image* of $\mathbf{x}$, and a point $\mathbf{x}$ such that $T(\mathbf{x}) = \mathbf{x}'$ is a *rank-1 preimage* of $\mathbf{x}'$.

If $\mathbf{x} \neq \mathbf{y}$ implies $T(\mathbf{x}) \neq T(\mathbf{y})$ for each $\mathbf{x},\ \mathbf{y}$ in S, then T is an *invertible map* in S, because the inverse mapping $\mathbf{x} = T^{-1}(\mathbf{x}')$ is uniquely defined; otherwise T is a said to be a *noninvertible map*, because points $\mathbf{x}'$ exist that have several rank-1 preimages, i.e. the inverse relation $\mathbf{x} = T^{-1}(\mathbf{x}')$ is multivalued. So, noninvertible means "many-to-one", that is, distinct points $\mathbf{x} \neq \mathbf{y}$ may have the same image, $T(\mathbf{x}) = T(\mathbf{y}) = \mathbf{x}'$.

Geometrically, the action of a noninvertible map can be expressed by saying that it "folds and pleats" the space S, so that distinct points are mapped into the same point. This is equivalently stated by saying that several inverses are defined for some points of S, and these inverses "unfold" S.

For a noninvertible map, S can be subdivided into regions $Z_k,\ k \geqslant 0$, whose points have k distinct rank-1 preimages. Generally, for a continuous map, as the point $\mathbf{x}'$ varies in $\mathbb{R}^n$, pairs of preimages appear or disappear as it crosses the boundaries separating different regions. Hence, such boundaries are characterized by the presence of at least two coincident (merging) preimages. This leads us to the classical definition of the *critical sets*, one of the distinguishing features of noninvertible maps (see [10,18]):

Definition. The *critical set CS* of a continuous map T is defined as locus of points having at least two coincident *rank* $-$ 1 preimages, located on a set CS_{-1}, called *set of merging preimages*.

This can be equivalently characterized[2] as the locus of points x' that are limits of sequences of points x'_n having preimage sets with more points than $T^{-1}(x')$.

The critical set CS is generally formed by $(n-1)$-dimensional hypersurfaces of $\mathbb{R}^n$, and portions of CS separate regions Z_k of the phase space characterized by a different number of *rank* $-$ 1 preimages, for example Z_k and Z_{k+2} (this is the standard occurrence for continuous maps). The critical set CS is the n-dimensional generalization of the notion of local minimum or local maximum value of a one-dimensional map, and of the notion of *critical curve LC* of a noninvertible two-dimensional map.[3] The set CS_{-1} is the generalization of local extremum point of a one-dimensional map, and of the *fold curve* LC_{-1} of a two-dimensional noninvertible map.

[2] We thank an anonymous referee for the suggestion of this definition.

[3] This terminology, and notation, originates from the notion of critical point as it is used in the classical works of Julia and Fatou.

Let us now consider the case of a continuous two-dimensional map $T : S \to S,\ S \subseteq \mathbb{R}^2$, defined by

$$T : \begin{cases} x_1' = T_1(x_1, x_2) \\ x_2' = T_2(x_1, x_2) \end{cases} \tag{12}$$

If we solve the system of the two equations (12) with respect to the unknowns x_1 and x_2, then, for a given $(x_1',\ x_2')$, we may have several solutions, representing rank-1 preimages (or backward iterates) of $(x_1',\ x_2')$, say $(x_1,\ x_2) = T^{-1}(x_1',\ x_2')$, where T^{-1} is in general a multivalued relation. In this case we say that T is noninvertible, and the critical set (formed by critical curves, denoted by LC from the French "Ligne Critique") constitutes the set of boundaries that separate regions of the plane characterized by a different number of rank-1 preimages. According to the definition, along LC at least two inverses give merging preimages, located on LC_{-1} (following the notations of Gumowski and Mira [10,18]).

For a continuous and (at least piecewise) differentiable noninvertible map of the plane, the set LC_{-1} is included in the set where $\det J$ changes sign, since T is locally an orientation preserving map near points (x_1, x_2) such that $\det J > 0$ and orientation reversing if $\det J < 0$. Of course, if the map is continuously differentiable then the change of the sign of $\det J$ occurs along points where $\det J$ vanishes, thus giving the characterization of the fold line LC_{-1} as the locus where the Jacobian vanishes.

For the map (2) the set LC_{-1} can be obtained by imposing $\det J_2 = 0$, where J_2 is given in (4):

$$LC_{-1} : 2a_{11}a_{21}x_1^2 + 2a_{12}a_{22}x_2^2 + (e_1a_{21} + 2e_2a_{11})x_1 + (e_2a_{12} + 2e_1a_{11})x_2 + 4a_{11}a_{22}x_1x_2 + e_1e_2 = 0 \tag{13}$$

which is a second degree equation, representing a conic in the (x_1, x_2) plane. The critical set LC is obtained by applying the map (2) to the conic (13): $LC = T(LC_{-1})$.

In order to give a geometrical interpretation of the action of a multi-valued inverse relation T^{-1}, it is useful to consider a region Z_k as the superposition of k sheets, each associated with a different inverse. Such a representation is known as *Riemann foliation* of the plane (see e.g. [10]). Different sheets are connected by folds joining two sheets, and the projections of such folds on the phase plane are arcs of LC. This is shown in the qualitative sketch of Fig. 11, where the case of a $Z_0 - Z_2$ noninvertible map is considered.

The graphical representation of the unfolding action of the inverses also gives an intuitive idea of the mechanism which causes the creation of non-connected basins, a property specific to noninvertible maps. We recall that the *basin*of an attractor A is the set of all the points that generate trajectories converging to A

$$\mathscr{B}(A) = \left\{ x | T^k(x) \to A \text{ as } k \to +\infty \right\} \tag{14}$$

If U is a neighborhood of A whose points converge to A (which exists by definition of attractor) then $U \subseteq \mathscr{B}(A)$, and *also the points which are mapped inside Uafter a finite number of iterations belong to* $\mathscr{B}(A)$, thus the *basin of A* is formed by all the preimages of the points of U

$$\mathscr{B}(A) = \bigcup_{j=0}^{\infty} T^{-j}(U) \tag{15}$$

where $T^{-1}(x)$ represents the set of the rank-1 preimages of x (i.e. the points mapped into x by T), and $T^{-j}(x)$ represents the set of the *rank* $-j$ preimages of x (i.e. the points mapped into x after j applications of T). Now, let us assume that $\mathscr{B}(A)$ is a connected basin for a given set of parameters, and as a parameter is changed $\mathscr{B}(A)$ has a contact with CS, after which a portion of $\mathscr{B}(A)$, say $\mathscr{B}_H$, crosses CS and enters a region Z_{k+2} with more preimages. This implies the creation of new portions of $\mathscr{B}(A)$ given by the new preimages $T_i^{-1}(\mathscr{B}_H),\ i = 1, 2$. If these preimages belong to regions Z_k, with $k > 0$, also other portions of $\mathscr{B}(A)$ are created after the contact, given by higher rank preimages of $\mathscr{B}_H$. So, the global bifurcations which transform a connected basins into a non-connected one can be explained in terms of *contacts of basin boundaries and critical sets*. Portions of the critical set CS and its images $CS_k = T^k(CS)$ can also be used to obtain the boundaries of trapping regions where the asymptotic dynamics of the iterated points of a noninvertible map are confined. In general, for an n-dimensional map, an *absorbing region* $\mathscr{A}$ (*intervals in R, areas in* R^2, *volumes in* $R^3, \ldots$) is defined as a bounded set whose boundary is given by portions of the critical set CS and its images of increasing order $CS_k = T^k(CS)$, such that a neighborhood $U \supset \mathscr{A}$ exists whose points enter $\mathscr{A}$ after a finite number of iterations and then never escape it, since $T(\mathscr{A}) \subseteq \mathscr{A}$, i.e. $\mathscr{A}$ is trapping (see e.g. [10] for more details). Inside an absorbing region one or more attractors may exist. However, if a chaotic attractor exists which fills up a whole absorbing region then the boundary of the chaotic attractor is formed by portions of critical sets. Following Mira et al.

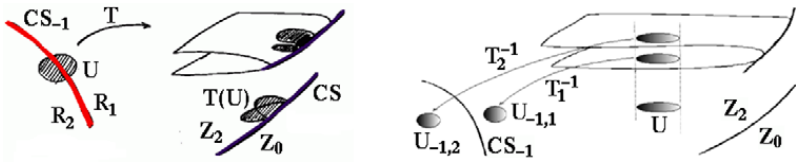

Fig. 11. Qualitative representation of the effects of the Riemann foliation.

[10] (see also Bischi and Gardini [29]) a practical procedure can be outlined in order to obtain the boundary of an absorbing area (although it is difficult to give a general method). Starting from a portion of LC_{-1}, approximately taken in the region occupied by the area of interest, its images by T of increasing rank are computed until a closed region is obtained.

Many of the considerations made above, for 2-dimensional noninvertible maps, can be generalized to n-dimensional ones, even if their visualization becomes more difficult. First of all, from the definition of the critical set it is clear that the relation $CS = T(CS_{-1})$ holds in any case. Moreover, the points of CS_{-1} where the map is continuously differentiable are necessarily points where the Jacobian determinant vanishes:

$$CS_{-1} \subseteq J_0 = \{p \in \mathbb{R}^n | \det J(p) = 0\} \tag{16}$$

In fact, in any neighborhood of a point of CS_{-1} there are at least two distinct points which are mapped by T into the same point. Accordingly, the map is not locally invertible in points of CS_{-1}, and (16) follows from the implicit function theorem. This property provides an easy method to compute the critical set for continuously differentiable maps: from the expression of the Jacobian determinant one computes the locus of points at which it vanishes, then the set obtained after an application of the map to these points is the critical set CS.

In the case of map (7) the set CS_{-1} can be obtained by imposing the condition $\det(J_3) = 0$, where J_3 is given in (8). What we obtain is a third degree equation with three variables. Of course, we can only manage it and its image $CS = T(CS_{-1})$ by numeric methods, with all the difficulties brought to light in Section 5, due to the problems of visualization of three-dimensional surfaces on a two-dimensional screen.

References

[1] Lotka AJ. Elements of physical biology. Baltimore: Williams & Wilkins Co.; 1925.
[2] Volterra V. Variazioni e fluttuazioni del numero d'individui in spece animali conviventi. Mem R Accad Naz dei Lincei VI 1926:2R.
[3] Goodwin RM. A growth cycle. In: Feinstein CH, editor. Socialism, capitalism and economic growth. Cambridge: Cambridge University Press; 1967. p. 54–8.
[4] Hofbauer J, Sigmund K. Evolutionary games and population dynamics. Cambridge: Cambridge University Press; 1998.
[5] Devaney RL. An introduction to chaotic dynamical systems. Menlo Park, California: The Benjamin/Cummings Publishing Co.; 1987.
[6] Mira C. Chaotic dynamics. From the one-dimensional endomorphism to the two-dimensional noninvertible maps. Singapore: World Scientific; 1987.
[7] Sharkovsky AN, Kolyada SF, Sivak AG, Fedorenko VV. Dynamics of one-dimensional maps. London: Kluwer Academic Publishers.; 1997.
[8] de Melo W, van Strien S. One-dimensional dynamics. Berlin-Heidelberg-New York: Springer-Verlag; 1991.
[9] Guckenheimer J, Holmes P. Nonlinear oscillations, dynamical systems, and bifurcations of vector fields. New York: Springer-Verlag; 1983.
[10] Mira C, Gardini L, Barugola A, Cathala JC. Chaotic dynamics in two-dimensional noninvertible maps. Singapore: World Scientific; 1996.
[11] Kuznetsov YA. Elements of applied bifurcation theory. 2nd ed. New York: Springer-Verlag; 1998.
[12] Agliari A, Bischi GI, Dieci R, Gardini L. Global bifurcations of closed invariant curves in two-dimensional maps: a computer assisted study. Int J Bifurcation Chaos 2005;15:1285–328.
[13] Blackmore D, Chen J, Perez J, Savescu M. Dynamical properties of discrete Lotka–Volterra equations. Chaos Solitons Fractals 2001;12:2553–68.
[14] Liu X, Xiao D. Bifurcations in a discrete time Lotka–Volterra predator–prey system. Discrete Continuous Dyn Syst – Ser B 2006;6:559–72.
[15] Liu X, Xiao D. Complex dynamic behaviors of a discrete-time predator–prey system. Chaos Solitons Fractals 2007;32:80–94.
[16] Bischi GI, Kopel M. Equilibrium selection in a nonlinear Duopoly game with adaptive expectations. J Econ Behavior Organ 2001;46:73–100.
[17] Agliari A, Bischi GI, Gardini L. Some methods for the global analysis of dynamic games represented by noninvertible maps. In: Puu T, Sushko I, editors. Oligopoly dynamics: models and tools. New York: Springer-Verlag; 2002. p. 31–83.
[18] Gumowski I, Mira C, Dynamique chaotique. Transition ordre-desordre, Cepadues, Toulouse; 1980.
[19] Puu T. Attractors, bifurcations and chaos. Berlin-Heidelberg-New York: Springer-Verlag; 2000.
[20] Bischi GI, Gardini L, Kopel M. Analysis of global bifurcations in a market share attraction model. J Econ Dyn Control 2000;24:855–79.
[21] Bischi GI, Mroz L, Hauser H. Studying basin bifurcations in nonlinear triopoly games by using 3D visualization. Nonlinear Anal Theory, Methods Appl 2001;47:5325–41.
[22] Hauser H, Mroz L, Bischi GI, Gröller E. Two-level volume rendering. IEEE Trans Visualization Comput Graphics 2001;7:242–52.
[23] Fortis M, Maggioni MA, Comportamenti sinergici e concorrenziali nello sviluppo di cluster industriali: una modellizzazione ecologica ed alcune evidenze empiriche, Complessità e distretti industriali: dinamiche, modelli, casi reali, Collana della Fondazione Edison, Il Mulino, Bologna; 2002.
[24] Gardini L, Lupini R, Mammana C, Messia MG. Bifurcations and transitions to chaos in the three-dimensional Lotka–Volterra map. SIAM J Appl Math 1987;47:455–82.
[25] Farebrother RW. Simplified Samuelson conditions for cubic and quartic equations. The Manchester School Econ Social Stud 1973;41:396–400.
[26] Gandolfo G. Economic dynamics: methods and models. Advanced textbooks in economics, vol. 16. Amsterdam, The Netherlands: North-Holland; 1980.
[27] Elaydi SN. An introduction to difference equations. New York: Springer; 1995.
[28] Okuguchi K, Irie K. The Shur and Samuelson conditions for a cubic equation. The Manchester School Econ Social Stud 1990;58:414–8.
[29] Bischi GI, Gardini L. Role of invariant and minimal absorbing areas in chaos synchronization. Phys Rev E 1998;58:5710–9.
[30] Dendrinos DS, Mullally H. Urban evolution studies in the mathematical ecology of cities. Oxford: Oxford University Press; 1985.
[31] Nijkamp P, Reggiani A. Interaction, evolution and chaos in space. Berlin: Springer-Verlag; 1992.
[32] Nijkamp P, Reggiani A. The economcs of complex spatial systems. Amsterdam: Elsevier; 1998.
[33] May RM. Stability and complexity in model ecosystems. Princeton NJ: Princeton University Press; 1973.
[34] Abraham L, Gardini L, Mira C. Chaos in discrete dynamical systems (a visual introduction in two dimensions). New York: Springer-Verlag; 1997.
[35] Mira C, Fournier-Prunaret D, Gardini L, Kawakami H, Cathala JC. Basin bifurcations of two-dimensional noninvertible maps: fractalization of basins. Int J Bifurcations Chaos 1994;4:343–81.
[36] Agiza HN, Bischi GI, Kopel M. Multistability in a dynamic cournot game with three oligopolists. Math Comput Simul 1999;51:63–90.